2017

Analysis of homogeneous charge compression ignition engine with emphasis on combustion timing and reaction rate

Arunim Bhattacharya

ABSTRACT

ANALYSIS OF HOMOGENEOUS CHARGE COMPRESSION IGNITION ENGINE WITH EMPHASIS ON COMBUSTION TIMING AND REACTION RATE

Arunim Bhattacharya, MS
Department of Mechanical Engineering
Northern Illinois University, 2017
Dr. Pradip Majumdar, Director

HCCI engines are a class of engines which use high compression ratio to ignite a charge of air-fuel mixture, essentially eliminating the need for spark plugs. This contrasts with diesel engines (although HCCI can be used for diesel engines) where the fuel is injected near the top dead center of the compression stroke regime. Gasoline HCCI engine is of significance because it attempts to improve the characteristics of the engine, for example the thermal efficiency. High compression ratio comes with higher thermal efficiency, yet the peak temperature remains low enough to have low production rates of harmful oxides of nitrogen and formation of soot. However, there are certain challenges associated with such type of engine, one of which and perhaps the most important of all is how to control the combustion rate. Flow dynamics and chemical-kinetics analysis, are essential to predict combustion timing, duration, and rate. The objective of this study is to analyze a HCCI engine using simulation analysis models including a three-dimensional CFD simulation model. Simulation analysis is carried out using a generic HCCI engine, initially with simplified chemical kinetics and using detailed chemical kinetics and RANS turbulence CFD model. A sensitivity analysis of the effect of rpm on the

combustion time, burn duration, heat release, efficiency and emission concentration is carried out.

NORTHERN ILLINOIS UNIVERSITY

DEKALB, ILLINOIS

DECEMBER 2017

ANALYSIS OF HOMOGENEOUS CHARGE COMPRESSION IGNITION ENGINE WITH EMPHASIS ON COMBUSTION TIMING AND REACTION RATE

BY

ARUNIM BHATTACHARYA

A THESIS SUBMITTED TO THE GRADUATE SCHOOL

IN PARTIAL FULFILLMENT OF THE REQUIREMENTS

FOR THE DEGREE

MASTER OF SCIENCE

DEPARTMENT OF MECHANICAL ENGINEERING

Thesis Advisor:
Pradip Majumdar

ACKNOWLEDGEMENTS

I would like to express immense gratitude to my advisor, Dr. Pradip Majumdar, for his continuous support and guidance throughout the whole research work and during my time as a master's student at NIU. I am thankful to my committee members, Dr. John Shelton and Dr. Nicholas Pohlman, for taking time out of their schedule to come to my proposal and defense and for providing their valuable inputs on the topic. I would also like to thank Dr. Federico Sciammarella for his willingness to support me from the department. I would also like to show my appreciation to Beatrice Kooken and Jeannie Peterson for their cooperation and valuable support during my graduate study at NIU.

Table of Contents

LIST OF FIGURES

Figure Page

LIST OF TABLES

Table Page

Chapter 1: INTRODUCTION TO HCCI

1.1 Background

As impetus for cleaner and greener environment intensifies so does the research for high-efficiency engines. A large part of the budget of an automaker goes into the research and development of reducing pollution and increasing efficiency. Traditionally companies have approached the problems by separately treating exhaust gas to reduce pollution and/or by increasing engine efficiency by adding ECUs to effect a more efficient combustion. However, for these cases the basic principle of producing work remains the same: a mixture of air and fuel is compressed and a spark is produced at the right time to induce combustion for gasoline engines, whereas for diesel engines, air is compressed to sufficiently small volume and fuel is injected at the right time to start combustion.

There exists another way to ignite air-fuel mixture, that has garnered significant momentum in the past few years as the limits of traditional methods have been reached. Compressing a mixture of air and fuel, for both petrol and diesel, until it auto-ignites is now under considerable focus of both researchers and automakers.

One such approach is the ***Homogeneous Charge Compression Ignition*** (HCCI) refers to a class of engines which have effectively done away with spark plugs, and instead use high compression ratio to ignite the homogeneous air-fuel mixture. The procedure is shown pictorially

in Figure 1. High compression ratio comes with higher thermal efficiency, yet the peak temperature remains low enough to have low production rates of harmful oxides of nitrogen and soot formation. However, there are certain challenges associated with such type of engine, one of which and perhaps the most important of all is how to control the combustion rate. Once the ignition occurs the reaction advances quite quickly and thus has high rate of pressure rise and high heat release rate. One technique is to induct exhaust gas recirculation (EGR) inside the combustion chamber to dilute the reactant mixture and subsequently lower the reaction rate and control emission formations.

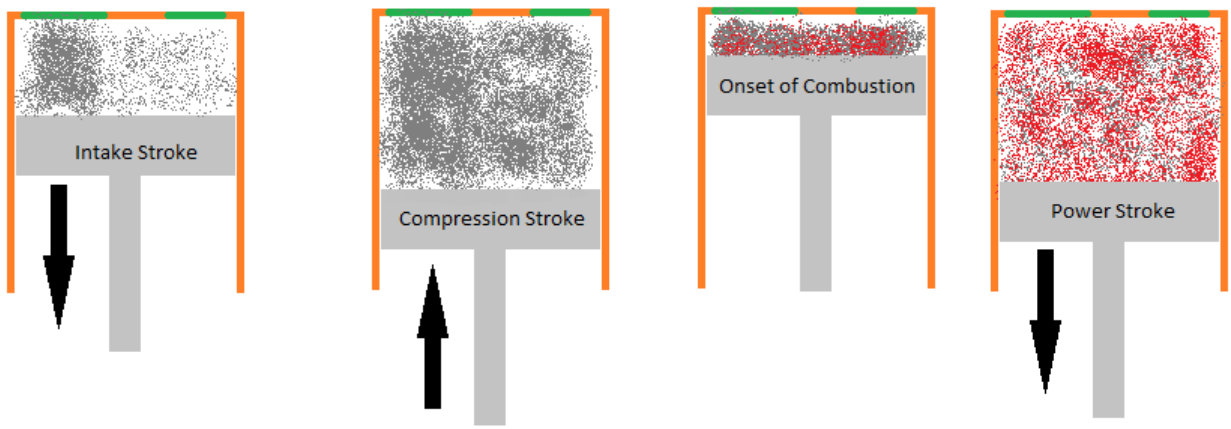

Fig. 1 Showing the HCCI process

Another method is to vary the temperature of intake mixture in conjunction with EGR to dilute the reactant mixture and subsequently lower the reaction rate and control emission. Raising the intake temperature leads to advancement of ignition and lowering leads to delayed ignition.

1.2 Literature

The idea behind HCCI engines is to reduce harmful pollutants and at the same time increase efficiency (Christensen et al., 1998). The latter is obvious because of the increased

compression ratio achieved by nature of operation. Reduced emission is a feature which was shown experimentally by Garcia and Aguilar (2009), using a modified diesel engine to work in HCCI model. The study by Garcia shows that formation of NOx, is significantly reduced when HCCI is operated with EGR as compared to Diesel with EGR, also HC emission is significantly increased for HCCI mode. However, the study involves injection of diesel fuel into partially compressed air inside the cylinder. The partially compressed air isn't hot enough to spontaneously ignite the fuel, so it allows for proper mixing for fuel and air. This arrangement allows for fuel adhering to cylinder walls and hence failing to ignite, which possibly gives rise to increased HC content in the exhaust. However, the model used in this study, intakes a homogenous mixture of air and fuel during the intake stroke. The idea behind it is that the combustion would be more complete, as ideally during the compression stroke pressure rise and temperature rise inside the cylinder space would be more uniform and hence combustion too would be uniform.

To predict the start and the end of combustion as well as rate combustion rate and mass fraction burn, a simplified approach based on Wiebe function distribution is often used instead of complicated reaction front computation approach. Yeliana et al. (2006) performed experimental analysis to established Wiebe function parameters based on pressure test data over arrange of operating conditions such as compression ratios and EGR rates. Yeliana (2006) demonstrated superior correlation with the experimental pressure tracing data using a double Wiebe function compared to the use of standard Wiebe function while using a single-zone combustion model.

Wang et al. (2006) performed 3D-CFD with detailed chemical kinetics analysis of direct injection gasoline HCCI engine to demonstrate the effect of two zone ignitions: fuel–rich zone

formed by second injection and the lean mixture zone formed by two consecutive injections on the ignition timing and combustion rate.

Woschni (1967) investigated the effect of piston speed and convection due to combustion on the heat transfer coefficient at the internal combustion engine wall. Functional forms to estimate local mean heat transfer coefficient in terms of parameters such as the piston motion, intensity of combustion, and number of experimental empirical constants are presented. Chang et al. (2004) performed experimental investigation of wall heat transfer coefficients in a HCCI engine based on wall temperature and heat flux measurement and compared with number of correlations including the one presented by Woschni. They presented a modified and improved version of the correlation applicable to HCCI combustion engine.

1.3 Objectives

The objective of this study is to understand the behavior of a HCCI engine and how it can be used to improve performance and reduce emissions. This study focuses mainly on the chemical kinetics to predict the combustion, first using a one-step global kinetics and then a CFD simulation for more refined results. Different analysis models are developed to predict the start of ignition for various equivalence ratios, estimate engine performance and pollutant levels, especially NOx, and gauge the effects of rpm on combustion.

Chapter 2: SIMULATION MODELS

Several simulation models are developed for analyzing HCCI engine combustion and engine performance. The first approach is a Wiebe function approach using a Simulink model where we estimate the mass fraction burn. The second approach includes simplified chemical kinetics but features no fluid dynamics. Third approach uses a combined computational fluid dynamics (CFD) model with complex chemical kinetics model.

2.1 Approach One: Wiebe Function/Simulink Model

A Simulink model was created to run preliminary simulations of HCCI engine. The model was developed around the popular Wiebe function equation. The Wiebe function (Yeliana,2006). is useful for estimating combustion of fuel without diving into complex chemical kinetics. It involves several parameters that necessitate experimental analysis to accurately determine their values. The most significant parameters are θ_0 , θ, which refers to start of combustion and duration of combustion respectively. Since knowledge of start of combustion is an essential parameter in the equation, this model is better suited to simulating spark-ignition (SI) engines. A single-function Wiebe function is given as follows:

$$x_b = 1 - \exp\left[1 - a\left(\frac{\theta-\theta_0}{\Delta\theta}\right)^{m+1}\right] \qquad \text{Eq. (2.1)}$$

where $a, m \ and \ \Delta\theta$ are Wiebe parameters that define the combustion characteristic and are define based on experimental data (commonly taken as 5 and 2).

The model was developed to get a qualitative understanding of the HCCI combustion. The model generates a set of piston position data which would be fed into the CFD software (Star CCM+) to be used to simulate different strokes of piston. This procedure helps in determining exact timing for opening and closing of valves. To truly simulate an HCCI engine, we need to resort to detailed chemical kinetics coupled with fluid dynamics. Simulink is a MATLAB tool which uses a graphical interface to build models. The advantage in using Simulink over traditional coding is that it provides several ways to display, modify and store data. There are pre-defined boxes available in the repository of Simulink, each of these boxes performs separate functions.

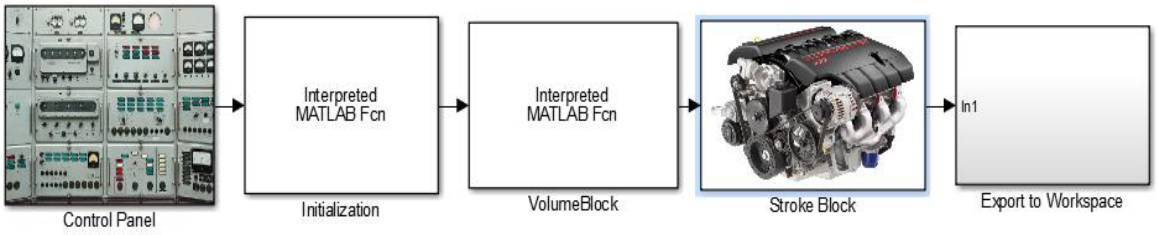

Fig. 2 Simulink blocks

Block 1 or Control Panel Block: This block sets the initial parameters (for example, equivalence ratio, burn time, ignition point, etc.) for a run of the simulation. Opening this block brings up the screen shown in Figure 3.

Block 2 or Initialization Block: This block does nothing but serve to feed the user defined parameters to the simulation itself. This block consists of a subroutine which captures the data from Block 1 and outputs them to the subsequent blocks.

Block 3 or Volume Block: This block calculates the volume inside an engine cylinder for a given crank angle.

Block 4 or Stroke Block: This is where the bulk of the calculation takes place, i.e., calculation of fuel consumption, pressure and temperature rise, etc. This block doesn't make use of chemical kinetics, rather it uses the Wiebe function.

Block 5 or Export to Workspace Block: Since Simulink doesn't automatically save its variables in MATLAB workspace, they must be saved explicitly using appropriate blocks.

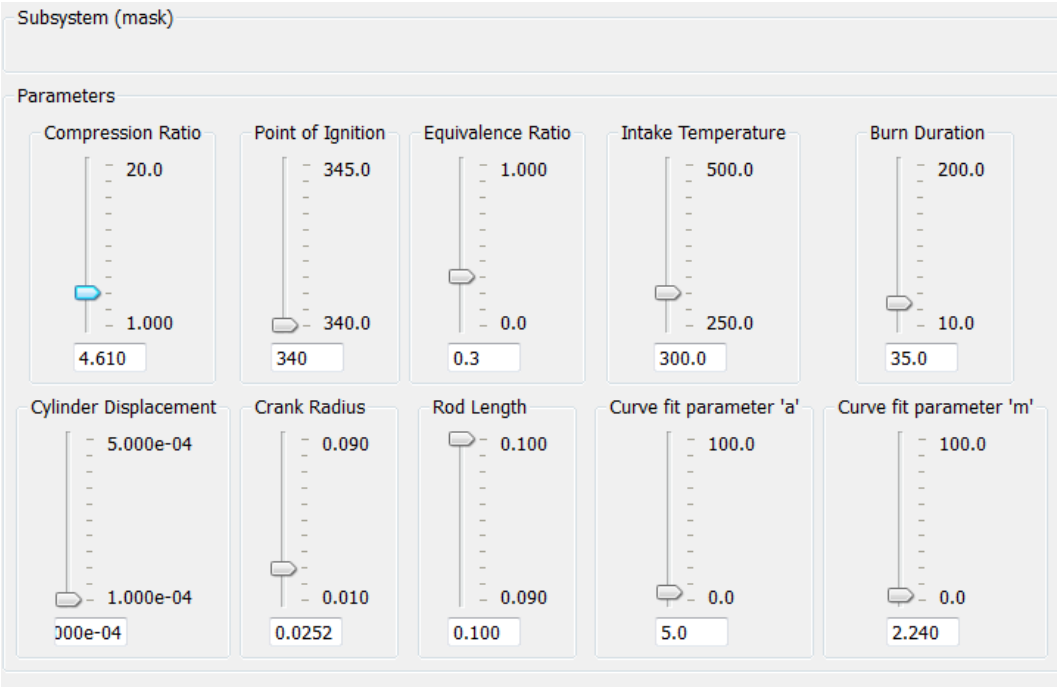

Fig. 3 Control panel block expanded view

2.2 Second Approach: Model with Simplified Chemical Kinetics

This second approach, is meant to be a step above the Simulink model since it includes chemical kinetics to simulate compression ignition. This analysis model features two cases: one neglects engine heat loss, and the second includes engine wall heat loss due to convection.

The chemistry used in this simulation is very much simplified as the essential idea is to get a quantitative understanding of the HCCI process. The chemical equation used for this combustion is as follows:

$$F + \upsilon Ox \rightarrow (1+\upsilon)Pr \qquad \text{Eq. (2.2)}$$

where F is the fuel, Ox is the oxidizer and Pr refers to the product. In this analysis, several assumptions have been taken besides the chemical equation and they are listed as follows:

- Molecular weights of oxidizer, fuel and products are considered same, i.e., 29 g.
- Molar specific enthalpy, ($\bar{c}_{p,I}$)was taken as a constant at 40 $\frac{J}{mol} - K$.

Equation 2.3 gives estimation of fuel consumption. The fuel of interest here is octane (C8H18).

$$\frac{d[C_8H_{18}]}{dt} = -Ae^{\left(-\frac{E_a}{R_uT}\right)}[C_8H_{18}]^m[O_2]^n \qquad \text{Eq. (2.3)}$$

where A is Arrhenius constant, E_a is activation energy. One thing to note here is that Equation 2.3 gives us the rate of change of concentration of the fuel which is expressed in moles/m3-s. Using molar concentration, we can determine the actual number of moles consumed at every instant and from there we can calculate the heat released. For this simulation, we used homogeneous reactor model, which essentially a quasi-isochoric process. The temperature and pressure rise using this method is given by the Equations 2.4 and 2.5.

$$\frac{dT}{dt} = \frac{\left(\frac{\dot{Q}}{V}\right) + R_uT\sum_i \dot{\omega}_i - \sum_i(\bar{h}_i\dot{\omega}_i)}{\sum_i[[X_i](\overline{c_{p,i}} - R_u)]} \qquad \text{Eq. (2.4)}$$

$$P = R_uT([F] + [Ox] + [Pr]) \qquad \text{Eq. (2.5)}$$

where T is the temperature of the gas mixture, $\dot{\omega}_i$ is the rate of fuel consumption, $\dot{Q}$ is the heat transfer to the system, and the quantities inside square brackets are species concentration.

2.3 Model with Global One-Step Chemical Kinetics and Wall Heat Loss

Building on the experience from the previous HCCI models and recognizing their drawbacks, we develop another model which includes calculation for heat loss at walls and uses the full-blown octane combustion equation. The engine parameters have been kept the same, however, since this model is reasonably accurate. There were some interesting results that were realized using this setup. The following equation:

$$C_8H_{18} + 12.5(O_2 + 3.76N_2) \longrightarrow 8CO_2 + 9H_2O + 47N_2 \quad \text{Eq. (2.6)}$$

2.3.1 Heat Release and Heat Transfer Model

The zero-order heat transfer model is derived by considering a conservation of energy over the control volume of the engine chamber. Combustion chamber is assumed to be a single-zone finite varying control volume composed of a perfect fuel-air mixture and with even distribution of the temperature pressure and concentration. Equation 2.7 is the energy equation used for the simulation. The first term on the left side of Equation 2.7 is the rate of heat release, the second term is rate of temperature rise, the third term is rate of work output, and the term on the right side is the heat loss through the wall. Equation 2.8 is algebraic form of the energy equation. The fuel consumption rate is given by Equation 2.3. A lumped capacitance overall energy balance including rate of reaction heat generation, engine work and rate wall heat loss lead to the following first-order transient heat equation:

$$n_f \bar{c}_p \frac{dT}{dt} = h_f \frac{dn_f}{dt} - \frac{d(PV)}{dt} - \frac{dQ_t}{dt} \qquad \text{Eq. (2.7)}$$

where:

n_f = moles

$\bar{c}_p$ = molar specific heat capacity of the mixture

h_f = enthalpy of combustion

Q_t = heat loss

$$T^{k+1} = \frac{\Delta n_f \bar{h}_f - T^k\left(R_u n^k - \bar{c}_p n^{k+1}\right) + A_r h_c T_w \, dt}{A_r h_c \, dt - R_u n^{k+1} + \bar{c}_p n^{k+1}} \qquad \text{Eq. (2.8)}$$

where:

Superscripts k, k+1 represent current and next time steps

A_r = surface area of cylinder for heat loss

h_c = heat transfer coefficient as calculated using Woschnii's relation

dt = time step

2.3.2 Heat Loss to Walls and Algorithm

The gas-to-wall heat transfer process in the engine is complex due to the interrupting nature of the turbulent boundary layer due to the varying motion of the piston during the compression and expansion strokes of the engine with the variation of the crank angle. The rate of heat transfer through all engine surface is given by the following equation:

$$\frac{dQ_t}{dt} = h_c \, A_r (T - T_w) \qquad \text{Eq. (2.9)}$$

where h_c is globally averaged convection heat transfer coefficient and T_w is cylinder wall temperature. A universally applicable equation for convection heat transfer coefficient was developed by Woschni (1967, 2009) for internal combustion engines taking into consideration the two predominant effects: (i) piston motion and (ii) convection due to combustion. The

correlation includes variation of number of operating variables such as gas temperature and pressure, cylinder diameter and experimentally determined empirical constants. In this zero-order analysis the following Woschni correlations is used.

$$h_c = 110 d^{-0.2} p^{0.8} T^{-0.53} \left[C_1 c_m + C_2 \frac{V_s T_1}{p_1 V_1} (p - p_m) \right]^{0.8} \quad \text{Eq. (2.10)}$$

Where:

C_1= 6.18 for 4th stroke, 2.28 2nd and 3rd strokes

c_m= Mean Piston speed

C_2 = 3.24x10-3 m/sec deg C

V_1= Volume at a known state

V_s= Cylinder displacement in m^3

Figure 4 shows the sequence of operations done in carrying out the simulation. Simulation is carried out over the following range of parameters: compression ratio-11-15; rpm 2000-5000; and equivalence ratio of 0.45.

2.4 Third Approach: Combined Computational Fluid Dynamics (CFD) with Complex Chemical Kinetics Model

Fluid flow dynamics, formation swirls and turbulence play a critical role on the engine combustion, heat loss, power output and emission formations. To consider these critical aspects on engine combustion and performance, this more comprehensive HCCI engine simulation model takes into account the flow dynamics of the fuel mixture and combustion products with the engine cylinder during motion of piston following the crank angle cycle.

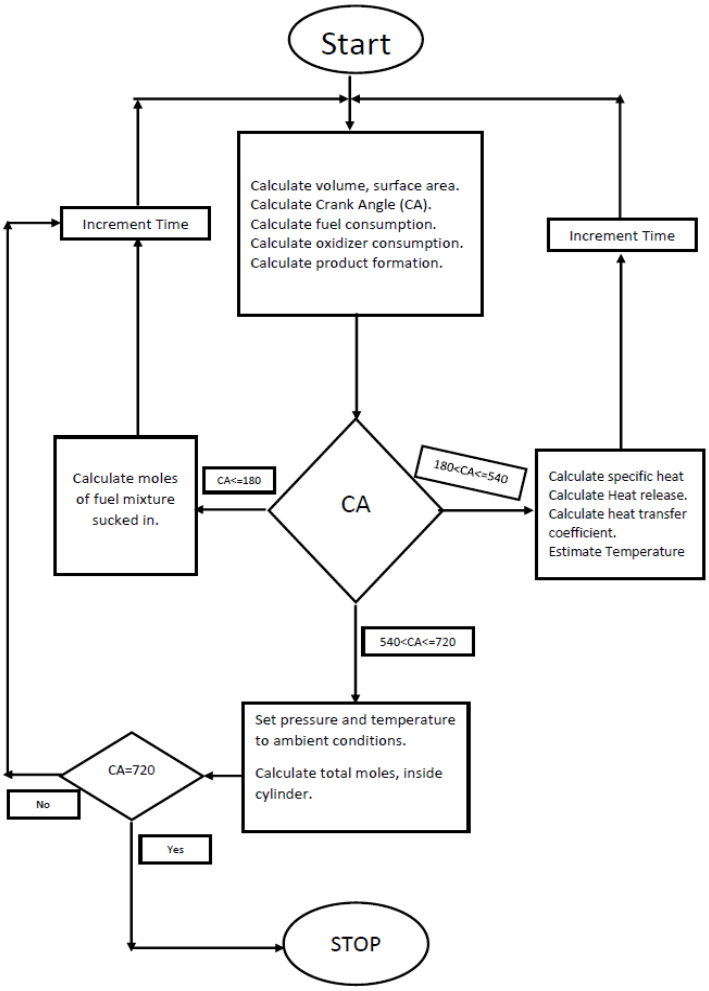

Fig. 4 Computational algorithm for one-step global kinetics

CFD model is then integrated with the advanced chemical kinetic model to predict the onset and rate of combustion, temperature and pressure rise and product species formation.

The CFD simulation was done in Star CCM+. The timing cycle estimated using the Simulink model is fed to the program to simulate different strokes. As the objective of this analysis is to understand the behavior of homogeneous combustion, the analysis was kept as simple as possible. The opening and closing of intake and exhaust valves are instantaneous; a more accurate modelling would have required use of dynamic fluid body interaction (DFBI). Physics models used are as follows:

- CVODE complex chemistry
- Gravity
- Implicit unsteady
- Species transport with binary diffusion
- RANS, realizable $k - \varepsilon$ turbulence model
- Segregated fluid enthalpy

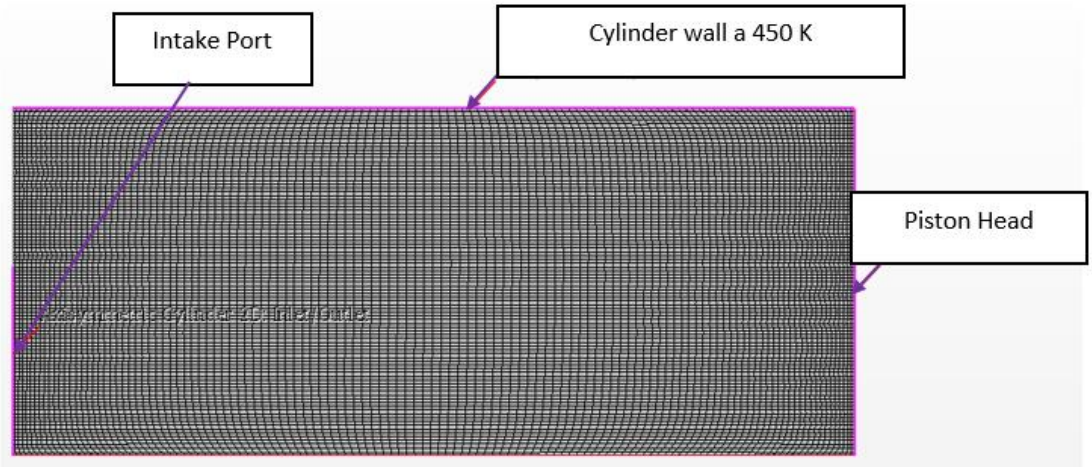

Fig. 5 Image shows the CAD model and mesh of 2D axisymmetric setup

- Zeldovich NOx model

Fig. 5 shows the axisymmetric model used in CFD simulation. A cylinder with flat piston head was selected to be used in the analysis. For greater clarity, different parts of the cylinder are numbered. Mesh chosen for this simulation is trimmer mesh with prism layer to capture the boundary layer. Trimmer mesh was chosen because it is easy to control the mesh density in different directions, making the mesh somewhat anisotropic. This was done as the mesh is supposed to deform in z-direction. Mesh chosen for this simulation is trimmer mesh with prism layer to capture the boundary layer.

2.4.1 Combustion

The previous chapters deal in the numerical method used for 0D simulation. The essential takeaway from the previous chapter is that to reduce the complexity we use a one-step global chemical equation to simulate the reaction. However, reaction occurs in multiple steps and on much smaller scale down to bimolecular reactions. This makes combustion simulation computationally very expensive. For example, combustion of octane can be represented by the following chemical equation:

$$C_8H_{18} + 12.5(O_2 + 3.76N_2) \longrightarrow 8CO_2 + 9H_2O + 47N_2 \qquad \text{Eq. (2.11)}$$

The fuel consumption rate for the above equation is given by the formula:

$$\frac{d[C_8H_{18}]}{dt} = -k[C_8H_{18}]^m[O_2]^n \qquad \text{Eq. (2.12)}$$

where *m* and *n* are indices determined experimentally and k is the reaction rate. This is a differential equation and solving it isn't complicated by any measure. However, if we care to break the combustion down to its individual reactions we will have something like following:

$$H_2 + O_2 \longrightarrow HO_2 + OH \qquad \text{Eq. (2.13)}$$

$$H + O_2 \longrightarrow OH + O \qquad \text{Eq. (2.14)}$$

$$OH + H_2 \longrightarrow H_2O + H \qquad \text{Eq. (2.15)}$$

$$H + O_2 + M \longrightarrow HO_2 + M \qquad \text{Eq. (2.16)}$$

From the above set of chemical equations, if we wish to derive the net rate of formation or consumption of O_2, we must take summation of formation /consumption rate of O_2 of all equations. The following equation is a mathematical interpretation of the above statement:

$$\frac{d[O_2]}{dt} = -k_1[H_2][O_2] - k_2[H][O_2] - k_4[H][O_2][M] \qquad \text{Eq. (2.17)}$$

where, k_1, k_2, k_4 are reaction rates of reactions 1, 2 and 3 respectively and the square brackets indicate concentration of a singular species in the gas mixture. Thus, we see that the equations to

keep track of various species become complex and computationally more expensive to solve. A typical chemical kinetics file contains hundreds of species and even more number of reactions.

This thesis uses sk171 chemical kinetics, which is a kinetics file for primary reference fuel (octane/heptane mix) combustion. This file is especially suited for simulating ignition under compression. For simulation of combustion we make use of a couple of files (Chemkin format) which contain information on the reactions and thermodynamics parameters for different species. Figure 2.5 shows a general schematic of how the combustion simulation works in Star CCM+.

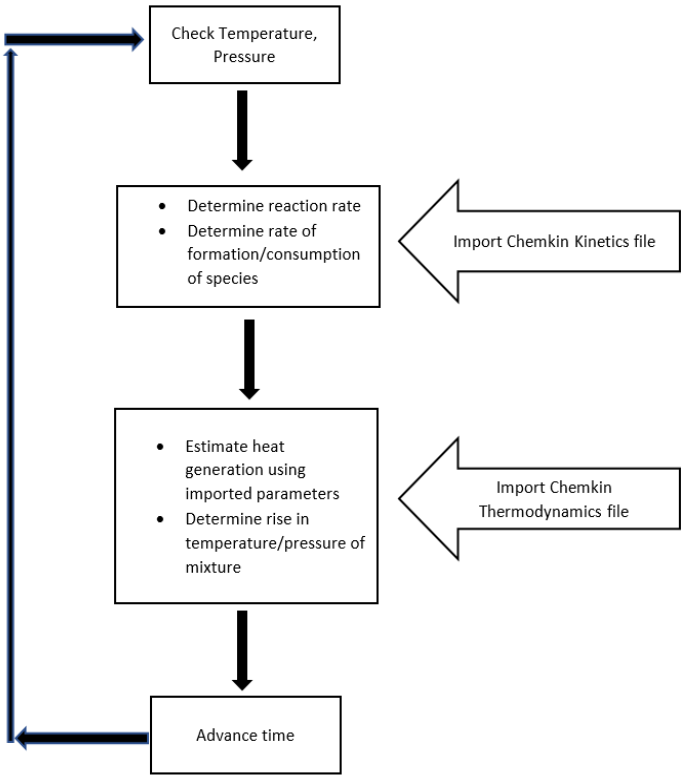

Fig. 6 Complex chemistry algorithm

As shown in Figure 6, Star imports two files to simulate combustion; the file which contains information about chemical kinetics (second step) is used to determine reaction rate for every chemical equation and then calculate rate of consumption/formation of species. Equation 2.17 shows an example formula on how to determine species formation rate; however, we need

to estimate the reaction rate first, which is denoted as $k_{1,2\ and\ 4}$. The chemical kinetics file contains individual reactions and its parameters like Arrhenius constant, activation energy, temperature index and pressure dependency. Reaction rate can be calculated by Arrhenius equation as follows:

$$k(T) = AT^{b}\exp(-\frac{E_a}{R_u T}) \qquad \text{Eq. (2.18)}$$

where *A, b, Ea, Ru* are Arrhenius constant, temperature index, activation energy and universal gas constant. Some reactions are reversible, and therefore the file also contains parameters for reverse reactions. Table 1 shows a few chemical equations and the parameters associated with it. Parameter *A* has the same unit as *k*, which in turn varies with the order of reaction.

Table 1 Chemical Kinetic Equations

Chemical reaction	**A**	**b**	**Ea** *(calories)*
H+O2<=>O+OH	3.547E+15	-0.406	1.660E+04
REVERSIBLE	1.027E+13	-0.015	-1.330E+02
OH+M<=>O+H+M	9.780E+17	-0.743	1.021E+05
REVERSIBLE	4.714E+18	-1.000	0.000E+00
CO+H2(+M) =>CH2O(+M)	4.300E+07	1.500	7.960E+04

At this point, I would like to mention the collision theory and how it relates to the Arrhenius equation. For a bimolecular reaction $A + B \rightarrow C + D$ we can write the rate of disappearance of species A as follows:

$$\frac{d[A]}{dt} = \left[\frac{\{Number\ of\ collisions\ between\ A\ \&B\}}{Volume.time}\right].[Probability\ of\ a\ collision\ leading\ to\ reaction].[\frac{1}{N_{AV}}]$$

Eq. (2.19)

Which in mathematical terms can be written as:

$$\frac{d[A]}{dt} = \left(\frac{Z_{AB}}{V}\right).\mathcal{P}.{N_{AV}}^{-1} \qquad \text{Eq. (2.20)}$$

where N_{AV} is Avogadro's number, $\mathcal{P}$ is the probability function, Z_{AB} is collision frequency between molecules species A and B, and V is volume. The probability, $\mathcal{P}$, of productive collision is defined as a function of two factors: energy factor i.e., $\exp[-\frac{E_a}{R_u T}]$, and a geometric factor, also called *steric factor*, ***p***. This factor considers geometry of a molecule to gauge the success of a collision and its value is typically less than 1.

$$\left(\frac{Z_{AB}}{V}\right) = \left(\frac{n_A}{V}\right)\left(\frac{n_B}{V}\right)\pi\sigma_{AB}^2.(\frac{8k_BT}{\pi\mu})^{1/2} \qquad \text{Eq. (2.21)}$$

where $n_{A,B}$ are number of molecules of species A and B, σ_{AB} is the sum of radii of molecules of A and B, k_B is Boltzmann's constant, and μ is defined as reduced mass. The final form of equation for consumption of species A can be written as follows:

$$\frac{d[A]}{dt} = pN_{AV}\sigma_{AB}^2.(\frac{8\pi k_BT}{\mu})^{1/2}\, exp\left[-\frac{E_a}{R_u T}\right][A][B] \qquad \text{Eq. (2.22)}$$

Thus, we see that the reaction rate can be written as follows:

$$k = AT^b\, exp\left[-\frac{E_a}{R_u T}\right] = pN_{AV}\sigma_{AB}^2.(\frac{8\pi k_BT}{\mu})^{1/2}\, exp\left[-\frac{E_a}{R_u T}\right] \qquad \text{Eq. (2.23)}$$

The second file that Star uses is the thermodynamics file. The thermodynamics file contains coefficient for the polynomial fit for enthalpy of formation, entropy and specific heat. The enthalpy of formation is what is used to determine heat generation. The following equations show the polynomial fit equations for the above properties:

$$\frac{Cp}{R} = a_1 + a_2T + a_3T^2 + a_4T^3 + a_5T^4 \qquad \text{Eq. (2.24)}$$

$$\frac{H^o}{R} = a_1 + \frac{a_2}{2}T + \frac{a_3}{3}T^2 + \frac{a_4}{4}T^3 + \frac{a_5}{5}T^4 + \frac{a_6}{T} \qquad \text{Eq. (2.25)}$$

$$\frac{S^o}{R} = a_1\ln T + a_2T + \frac{a_3}{2}T^2 + \frac{a_4}{3}T^3 + \frac{a_5}{4}T^4 + a_7 \qquad \text{Eq. (2.26)}$$

where, Cp, H^o, S^o, R, T and $a_{1,2\ldots}$ are specific heat, enthalpy of formation, entropy, universal gas constant temperature, and curve fit coefficients respectively. Table 2 shows the coefficients for a few of the species.

Table 2 Curve Fit Coefficients for Different Species Between Temperatures of 300K and 1000K

Species	a1	a2	a3	a4	a5	a6	a7
H	0.025e+02	0	0	0	0	0.0255E+06	-0.05E+01
HO2	4.0172109	2.239E-03	-6.34E-07	1.142E-10	-1.08E-14	1.1185E+02	3.785102
CH2CO	0.0604E+02	0.058E-01	-0.02E-04	0.028E-08	-0.02E-12	-0.086E+05	-0.08E+02

Star CCM+ offers two choices for the solution of combustion equations. One is CVODE method, the other one is DARS. The method used in this thesis is CVODE. CVODE is essentially a solver for a system of ordinary differential equations. There are as many ODEs as there are species.

Chapter 3: RESULTS AND DISCUSSIONS

The chapters preceding to this, deal with the description and setup of various models for HCCI engine combustion, performance and emissions. This chapter aims to present results obtained from the simulations. The order of presentation of the results is kept in sync with the order of the models presented in Chapter 2. Thus, we first discuss the results from the Simulink model and then we move on to discussing the results for 0D chemical model. At last we talk about the CFD model.

3.1 Approach One: Wiebe Function/Simulink Model

Figures 7 and 8 show the variation of the HCCI engine performance with increase in equivalence ratio, which represents the richness or amount excess air in the mixture. This is defined as:

$$\Phi = \frac{(A/F)_{Sto}}{(A/F)} \qquad \text{Eq. (3.1)}$$

where,

$(A/F)_{Sto}$= stoichiometric air- fuel ratio with no excess air for combustion

(A/F) = actual air-fuel ratio with excess air

A value of $\Phi < 1$ represents a fuel-lean mixture

Figures 7 and 8 show the variation in engine work output and efficiency with increase in the equivalence ratio (phi) in the range of 0.3-1.0 respectively. Results show that the work done increases with increasing equivalence ratio in a linear manner as expected.

ratio. efficiency dropped from 55% to about 52.5% as the Equivalence ratio increased from 0.3 to 1, i.e., as the fuel becomes less lean. The figure 8 shows the effect of burn duration on engine efficiency for different equivalence ratio.

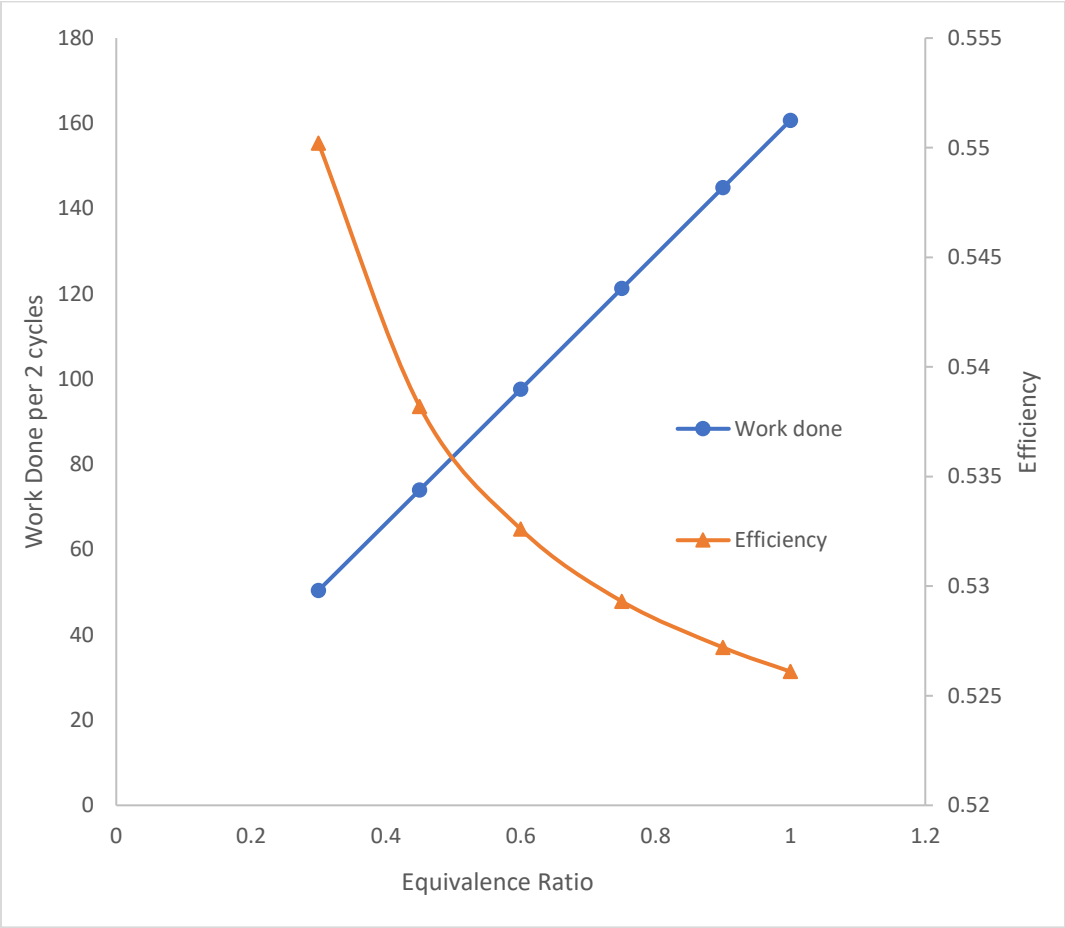

Fig. 7 Variation in Work output and efficiency with Equivalence Ratio

Figure 8 shows the variation of thermal efficiency vs burn duration in terms of crank angle variation (measured in degrees) and with Equivalence Ratio. The plot shows that there exists an optimal spot for every value of equivalence ratio where the efficiency is the highest. In this case it is about 25 degrees of burn duration. Also, it shows a direct increase in thermal

efficiency with the decrease in Equivalence Ratio. This data though only a crude estimate, can be used to get a qualitative idea of the optimum parameters for an engine.

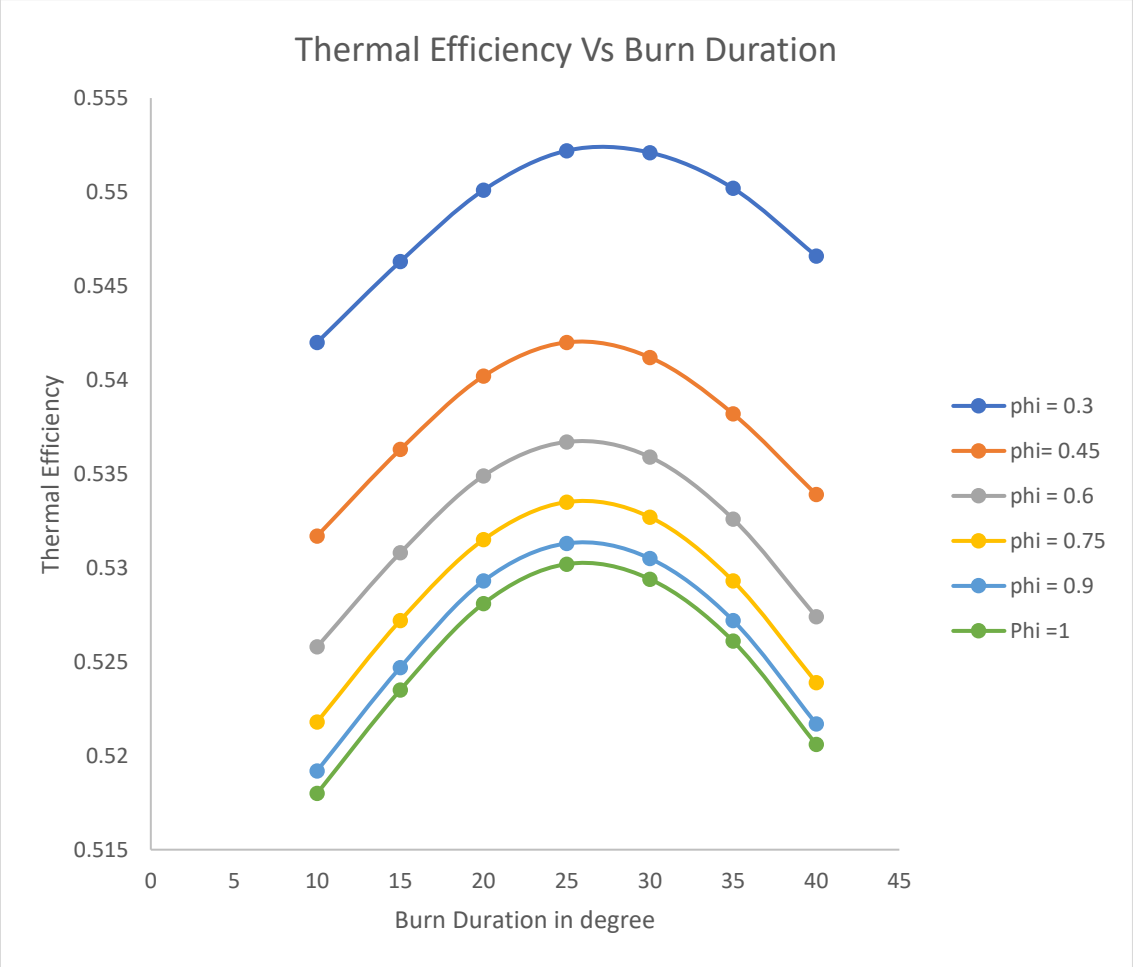

Fig. 8 Variation in efficiency with burn duration and equivalence ratio

Figure 9, shows the variation of net work output with of crank angle variation and with equivalence ratio. As expected, the work output is maximum at the point of maximum efficiency. However, we note that for very lean mixtures the difference in peak work output and shallow work output is quite insignificant.

Figure 10 shows a plot of peak temperature vs burn duration for different equivalence ratios. At first glance, we note that the peak temperature is a strong function of the equivalence ratio, i.e., higher the equivalence ratio, the higher is the overall peak temperature. Figure 11 shows the pressure plot at equivalence ratio of 1.0 and compression ratio of 13.

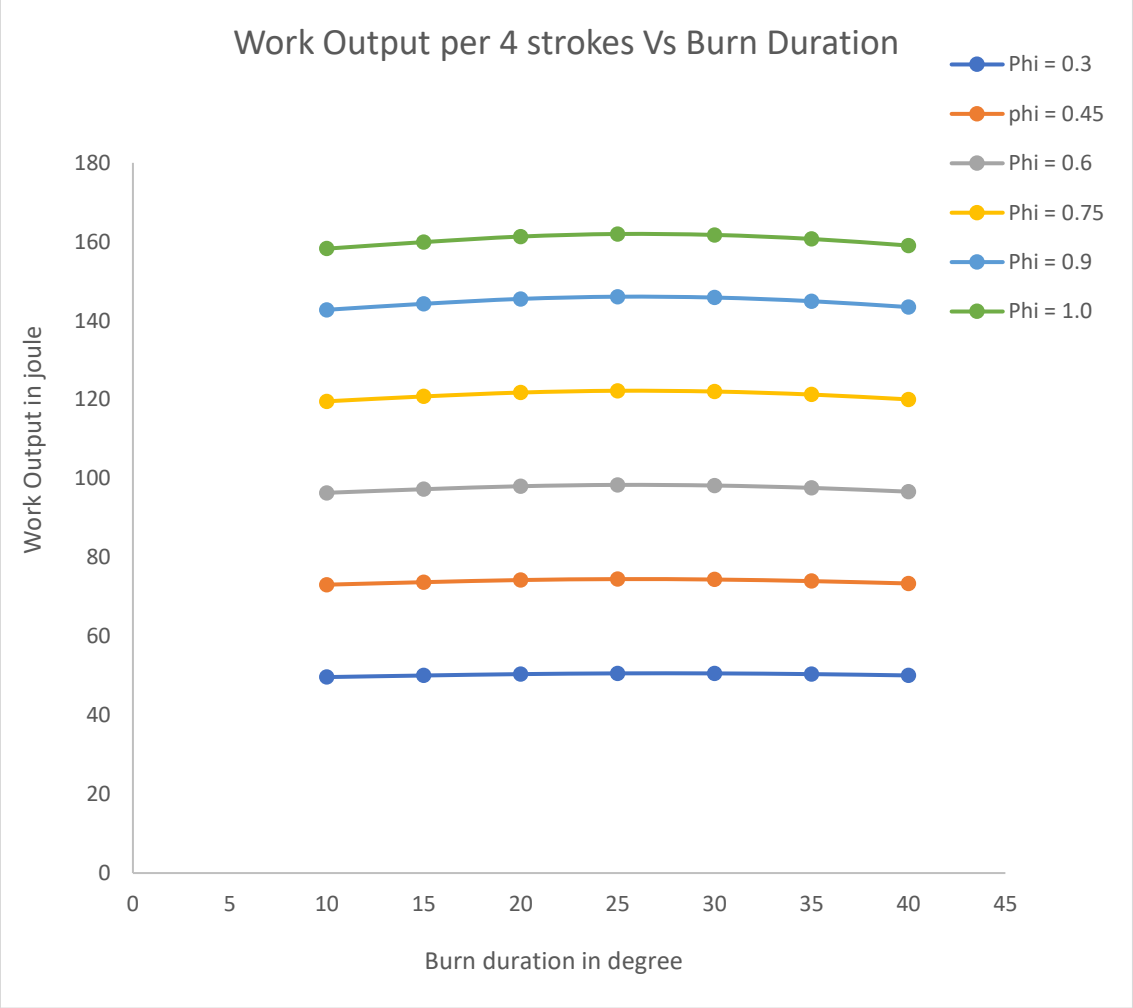

Fig. 9 Variation of work output with of crank angle variation and with Equivalence Ratio

Peak temperature is an important consideration for engine design because high temperatures are sources of large thermal stresses and risk melting of the constituent metals, yet another aspect that is important, especially for this report, is the production of oxides of nitrogen.

Formation oxides of nitrogen are significant only when the temperature inside combustion chamber is high.

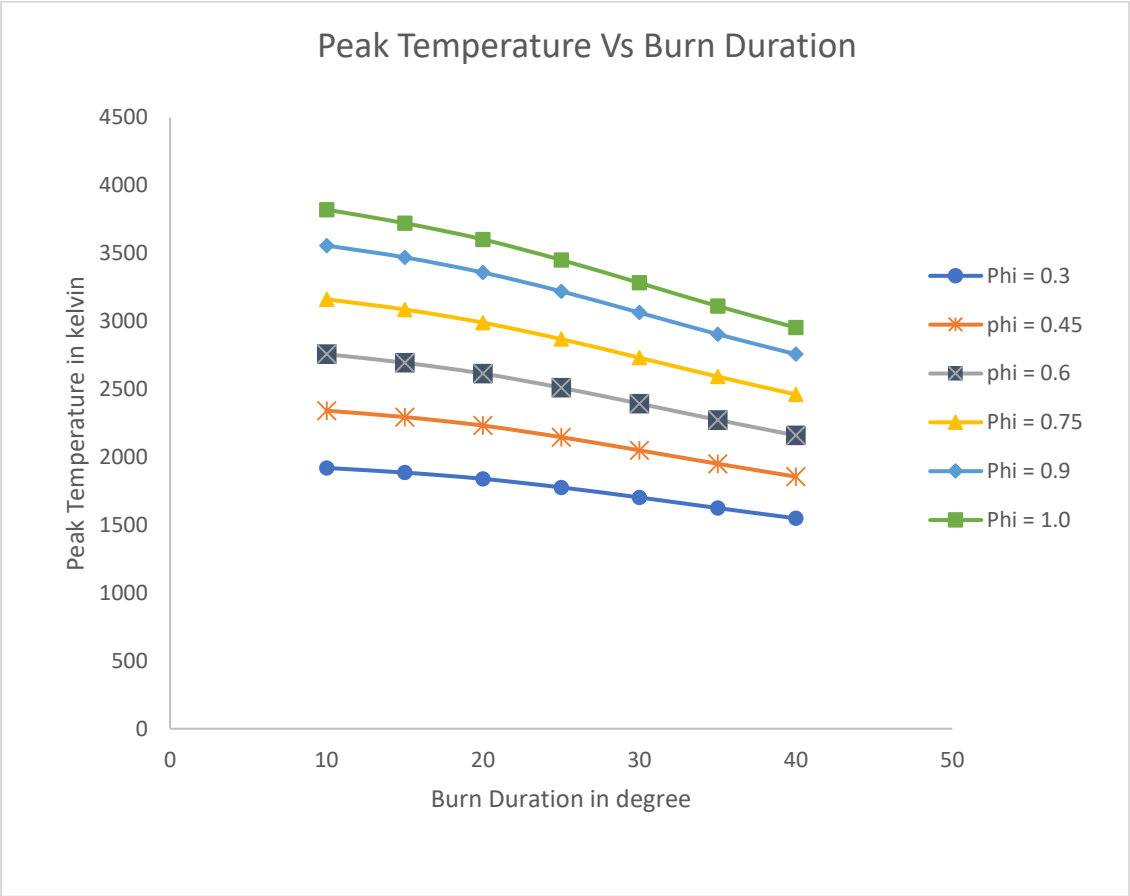

Fig. 10 Variation in peak temperature vs burn duration for different equivalence ratios.

Usually nitrogen is treated as an inert gas for low temperatures; however, it becomes reactive at high temperatures; from Figure 10 plot, it is interesting to note that burn duration significantly affects the peak temperatures, i.e., higher the duration, the lower is the peak temperature. This effect is more pronounced at higher equivalence ratios.

Some of the limitations of this approach are: 1. The heat release is dependent on factors that don't include chemical kinetics. 2. Wiebe function parameters must be determined

experimentally and are unique to every engine. 3. Nature of the equation makes it better suited to spark-ignition engines.

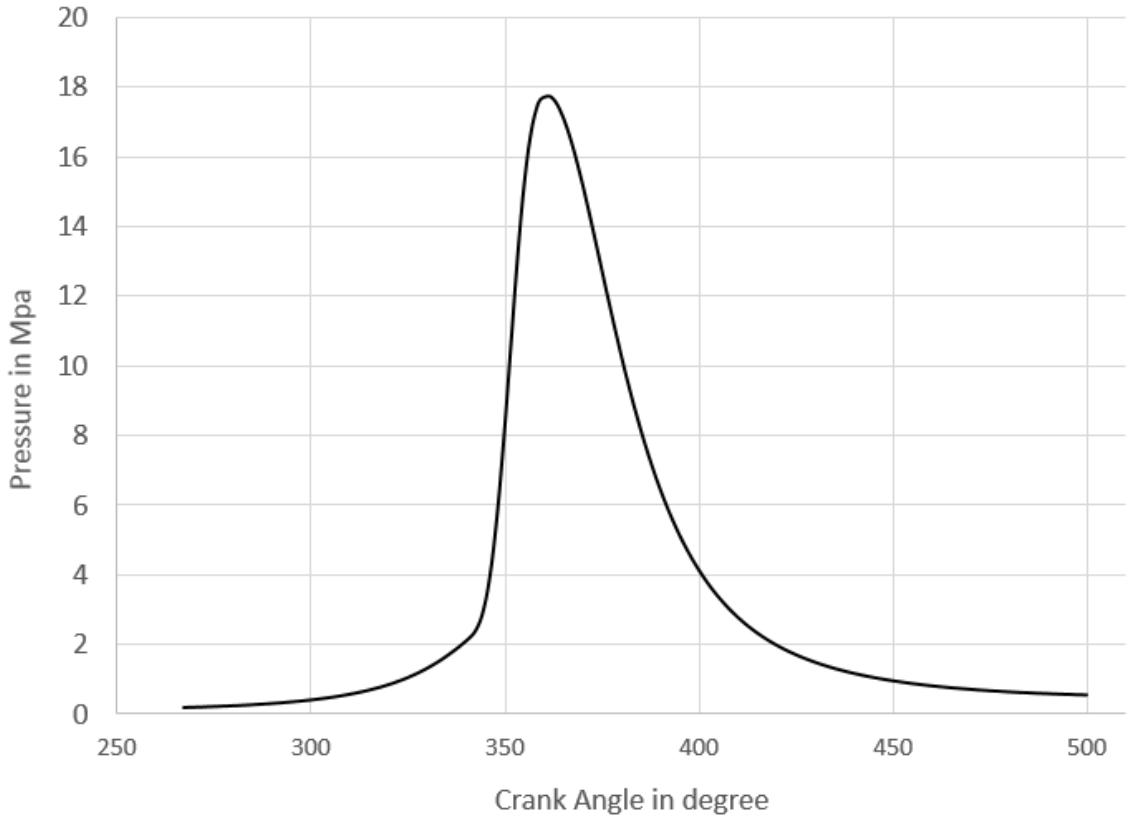

Fig. 11 Pressure vs Crank angle at equivalence ratio of 1

It can be noted here that it is difficult to control the burn duration. However there exists ways to effectively retard the rate of reaction, for example by using exhaust gas recirculation which in effect reduces the concentration of the reactants and hence retards the reaction. The values estimated in the above model are generally over predictions (true for all the plots in this chapter) of real-world values. The reason is that the model uses reversible adiabatic assumption. So essentially it doesn't consider the frictional effect and ignores the effect of the coolant on the engine cylinder. Apart from the above inferences, this model was used to estimate the exact moments of opening and closing of intake and exhaust valves.

3.3 Third approach: Model with Chemical Kinetics and Heat Loss

This simulation analysis models includes following basic steps: i). Deciding on a chemical equation; ii). Estimate concentration of reactants, and thus reaction rate; iii). Estimate heat release and temperature rise using constant volume-fixed mass reactor concept; and iv). Update concentration of reactants.

Since auto-ignition is so rapid, the heat release plots resemble that of a delta function. Onset of combustion and duration of burning varies significantly with the rpm. Figures 12 and 13 show the variation of temperature and pressure in the engine cylinder respectively for different. rpm.

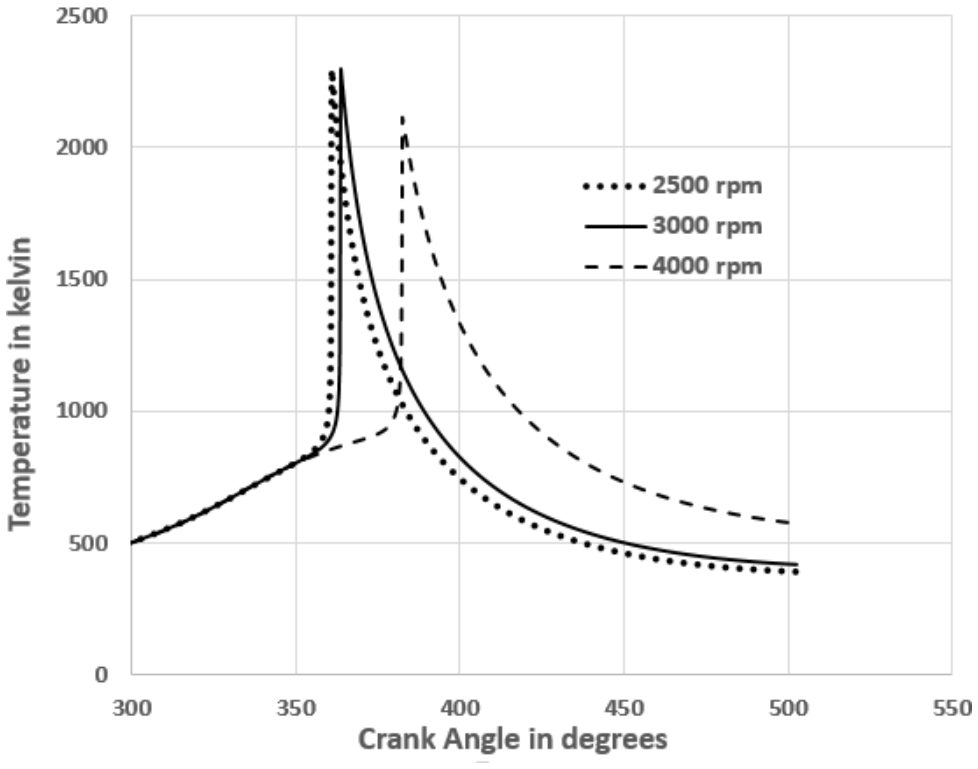

Fig. 12 Temperature variation vs crank angle

Results show onset of combustion around 360 crank angles and causing peak temperature reaching around 2250 K at around 360 of crank angle for both 2500 and 3000 rpm. A delayed

combustion is, however, noticed with further increase in rpm to 4000 and resulted in a lower engine peak temperature of 2100 K.

The pressure plots show a peak pressure rise to 10 MPa at 360-degree crank angle for 2500 rpm and 300 rpm. A significantly reduced peak pressure rise to 6 MPa is seen for 4000 rpm.

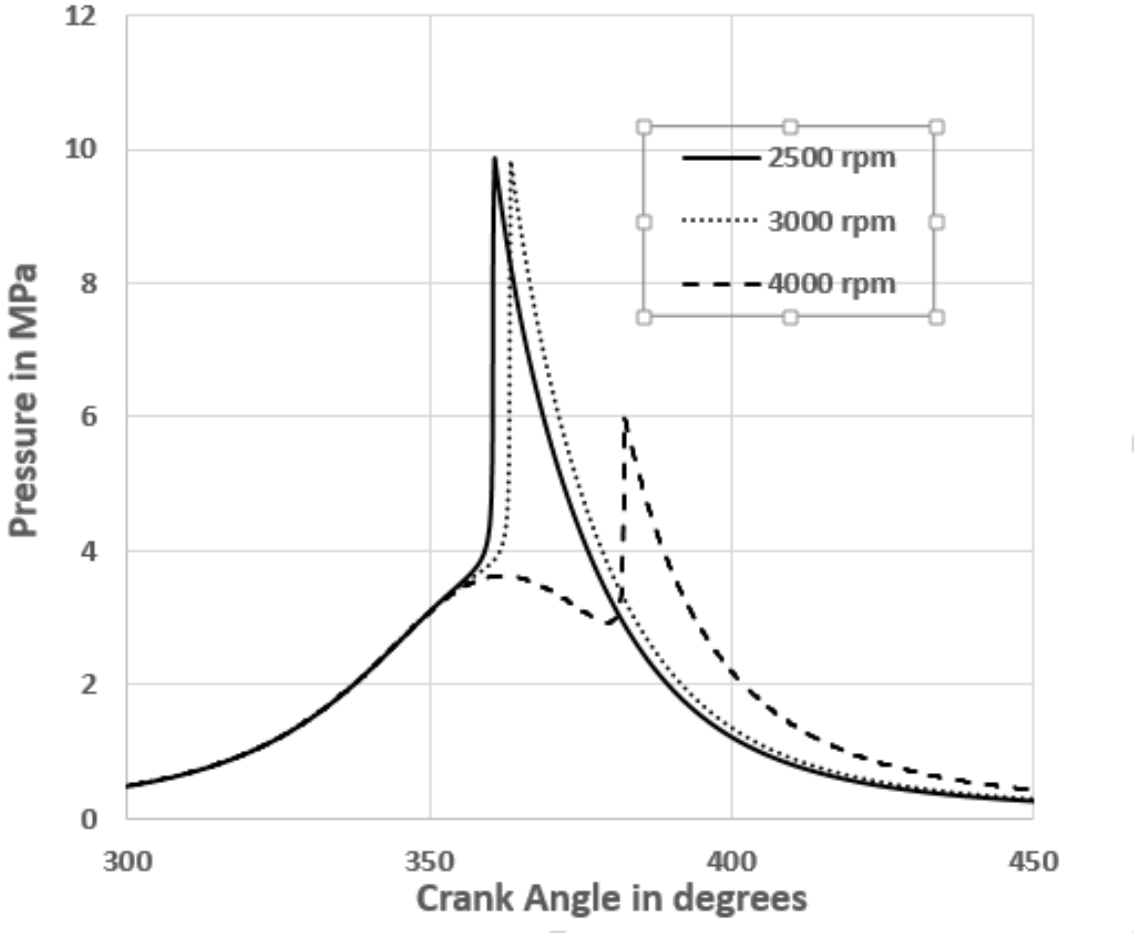

Fig. 13 Temperature variation vs crank angle

Figure 14 shows the variation of work output for various compression ratios for a range of rpms. We note that for a given rpm, there exists an optimum compression ratio where the work output and hence efficiency is highest and that the net work output decreases whenever we exceed that sweet spot. However, we also observe that for a given compression ratio, higher rpm

gives us higher work output. The zero-order simulation, although it has deficiencies, provides us with a qualitative understanding of the behavior of a HCCI engine.

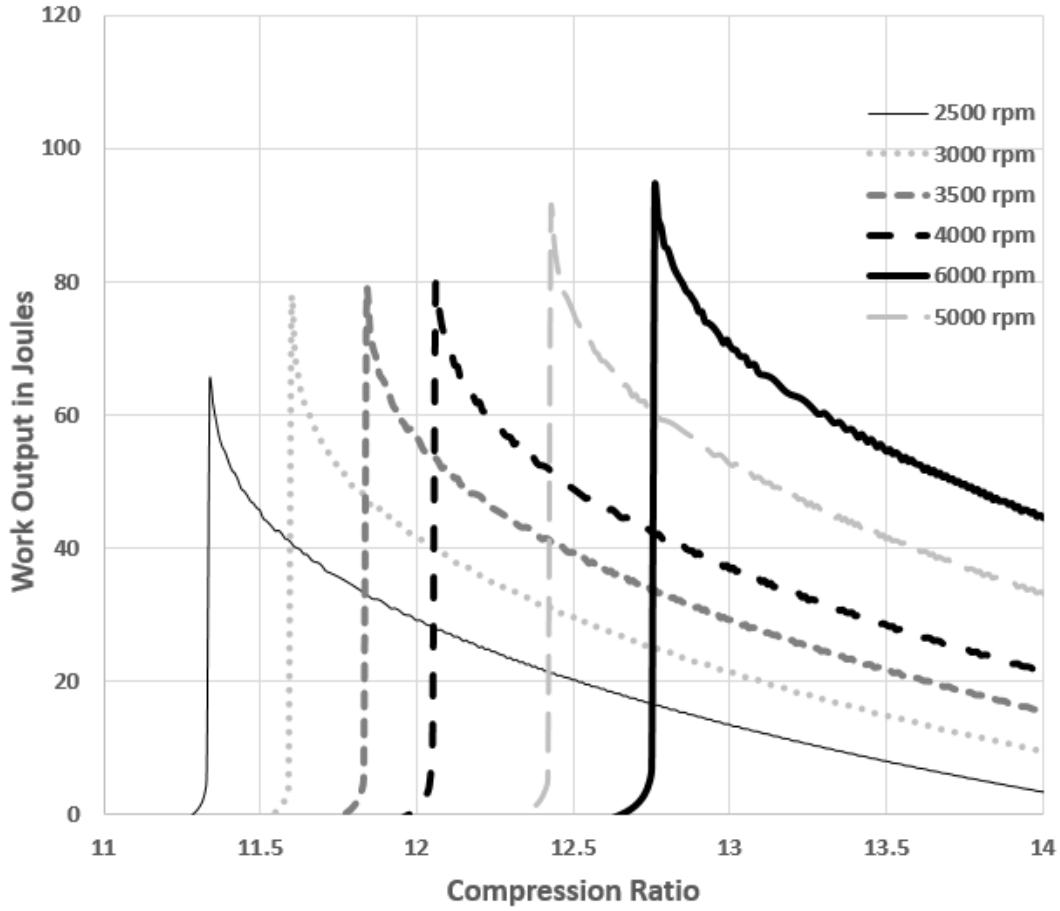

Fig. 14 Temperature variation vs crank angle

Figure 15 shows us the fuel burn duration at different rpm. The higher the rpm, higher is the fuel burn duration. In fact, what we observe is that slower the burn, higher is the work output. If we look at Figure 13 we see that the curve for 4000 rpm is a bit peculiar; the pressure decreases after crank crosses 360^{o}, whereas the other curves increase sharply after 360^{o}.However looking at the temperature plot (Figure 12) and the fuel burn plot (Figure 15) tells us that fuel keeps burning and temperature keeps rising, albeit at a more gradual pace. However, at about 380^{o} CA we observe a sharp rise in temperature, pressure, and consumption of fuel.

The objective of HCCI engine is to bring down the formation of pollutants, especially NOx, while increasing efficiency. Slow burning of fuel helps in doing just that by reducing the peak temperature and pressure while at the same time increasing work output. One of the well-known ways to do that is by inducting exhaust gases to the combustion chamber, it serves to retard the combustion and subsequently decreases peak pressure and temperature. Figure 16 shows a typical instantaneous heat transfer plot.

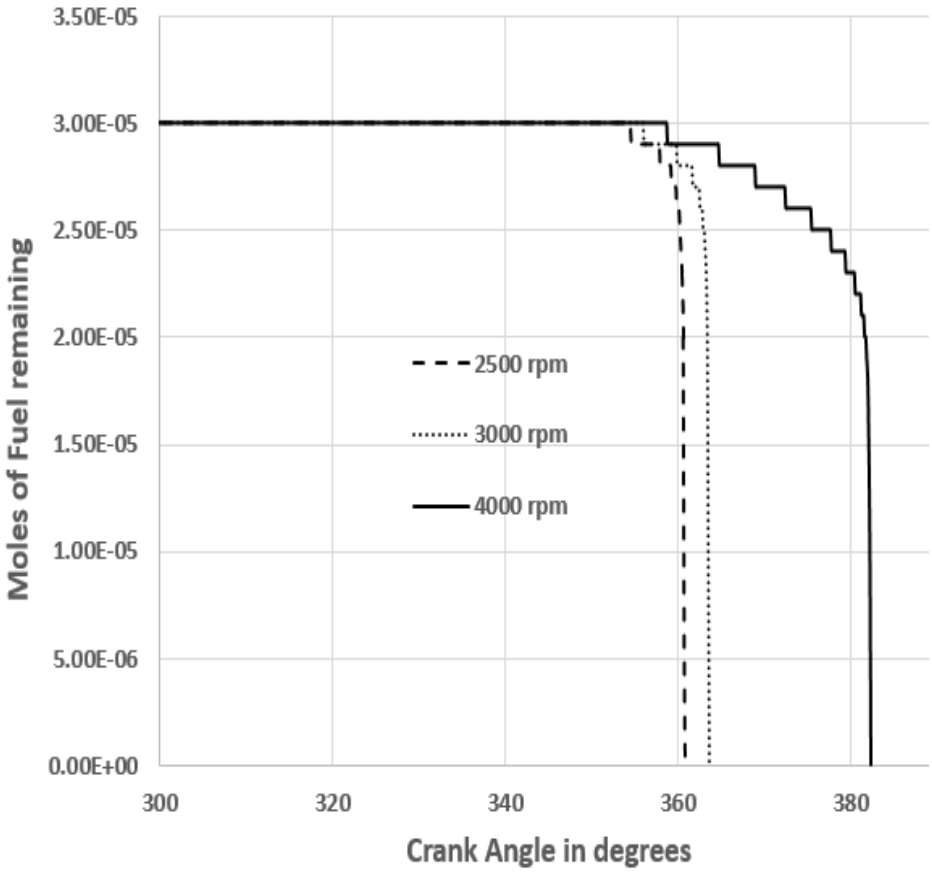

Fig. 15 Burn duration for different rpm

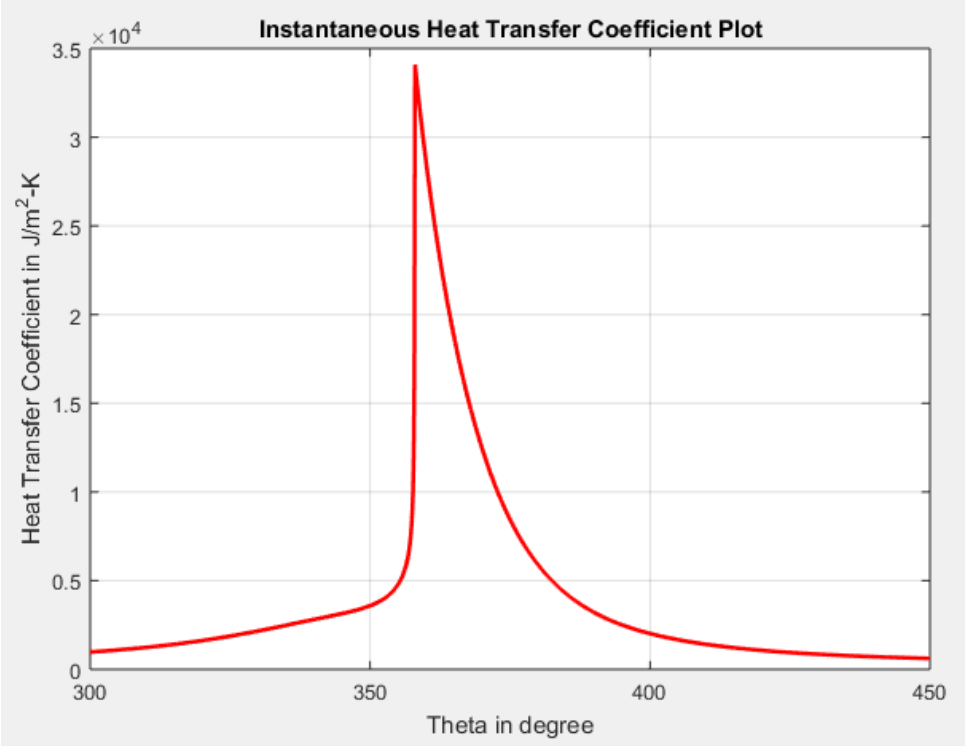

Fig. 16 Heat transfer coefficient plot

Chapter 4: CFD MODEL

Models described in previous chapters deal with HCCI combustion purely from chemical kinetics standpoint, which is termed as 0D models as they don't account for spatial variation. We consider the mixture inside the cylinder to be truly homogeneous. However, the downside to estimating a fully homogeneous behaviour is that combustion occurs simultaneously, throughout the cylinder because it assumes uniform temperature. There is a necessity to have a better approximation of the physics involved if we wish to understand the HCCI behavior. Therefore, CFD simulation is a natural progression in this regard. This chapter deals purely in the CFD treatment of the HCCI concept.

4.1 Setup of 2D Axisymmetric and 3D Models

CFD models are generally quite computationally expensive, thus it is often a better idea to start off with a less computationally expensive 2D model; in this case we use an axisymmetric model. The idea behind it is that, once the physics of the problem are figured out, it is only a matter of scaling to another axis. Also, another point worth mentioning is that, since we are using complex chemical kinetics and since it too is heavy on CPU, starting off with a 2D simulation is a better idea.

Figure 5 shows the mesh and the 2D model used in the simulation. Due to the nature of the setup, we had to position the intake port at the center as shown in the figure. The cylinder wall is kept at 450k and the wall on extreme right is setup as the piston head. The mesh used in this was purposefully chosen to have an optimum control over the aspect ratio of the deforming

volume. The representation shown in Figure 5 is at its maximum volume; however, the mesh operation is performed over a much smaller volume which is 1/18.4 (compression ratio) of the maximum size, so care had to be taken to ensure the nodes didn't get stretched too far out in the x direction, considering y as the vertical and x as the horizontal axis. Table 3 summarizes a few of the parameters used for CFD modelling.

Table 3 Model Comparison

PARAMETER	CFD (2D AND 3D)	0D
CYLINDER VOLUME	100 cc	100 cc
INTAKE TEMPERATURE	450 K, 300K	300 K
CYLINDER WALL TEMPERATURE	450K	450K
CHEMICAL KINETICS	Sk171 Complex	Global 1-step
COMPRESSION RATIO	18.4	13

The CFD analysis must be expanded to three dimensions to obtain conclusive results on the subject. As pointed out earlier, 3D simulations are computationally quite expensive, especially when simulation involves complex chemical kinetics. In the study here, we run the simulation over half of the total volume, bisecting intake and exhaust ports. The bisecting plane is treated as a plane of symmetry. Figure 17 shows the 3d model; one will notice that the intake port diameter is significantly larger than the exhaust port diameter. This is so because the intake is achieved at atmospheric pressure, so a large area is required to achieve a good overall suction of fuel-air mixture. The exhaust port can be made smaller since the exhaust gas is typically under high pressure. The 2D model differs from the 3D in the placement of intake port (for 2D exhaust

and intake share the same port); all other aspects have been kept the same. Mesh shown in the Figure 17 is trimmer mesh, with four prism layers to capture the boundary layer. The mesh is coarse in x and y axes whereas relatively fine in z direction (z being directed downwards from the ports).

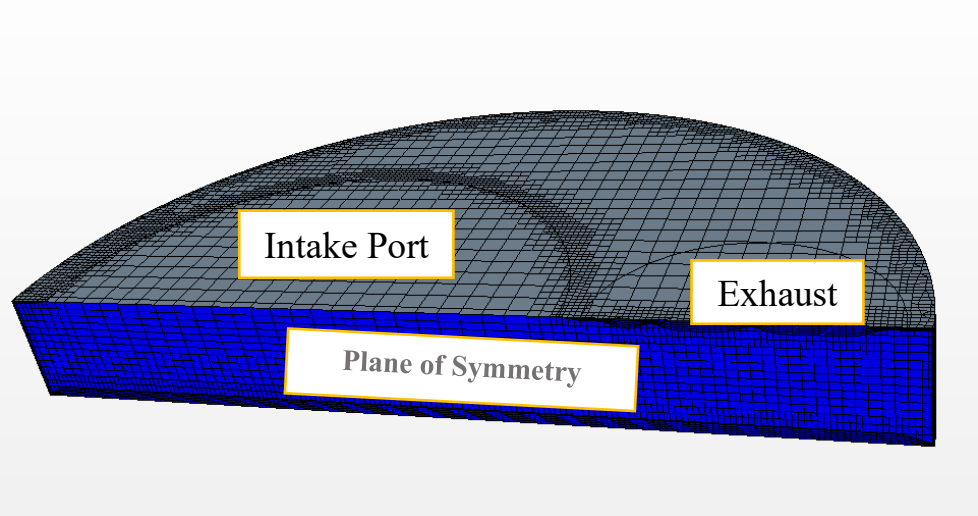

Fig. 17 Geometry and Mesh

The following lists physics incorporated into the solution:

- CVODE complex chemistry (sk171)
- Gravity
- Implicit unsteady
- Species transport with binary diffusion
- RANS, realizable $k - \varepsilon$ turbulence model
- Segregated fluid enthalpy
- Zeldovich NOx model

The sk171 chemistry model doesn't include NOx formation chemistry, so we used the Zeldovich NOx (nitric oxide only) model, which is available inside the Star CCM+ software. The Zeldovich model depends on high temperature to kick in. It is in our best interest to keep the peak temperature as low as possible to curb its production. The formation of NO is expressed in three steps as follows:

$$N_2 + O \rightarrow NO + N \quad \text{Eq. 4.1}$$

$$N + O_2 \rightarrow NO + O \quad \text{Eq. 4.2}$$

$$N + OH \rightarrow NO + H \quad \text{Eq. 4.3}$$

The heat loss at wall uses a conjugate heat transfer model and is kept at a steady 450K. The turbulence model was chosen based on Zhang's paper (Zhang, Kung, & Haworth, 2005), where the authors surmise that k-epsilon model is accurate enough for HCCI simulation. As will be shown later, the combustion is slow to start, but it picks up pace very rapidly. To capture the peak temperature, we slow down the time step to two hundred thousandths of a second; this also ensures the stability of solution during the peak of combustion.

4.2 Axisymmetric Results

Figure 18, gives an indication of how the combustion progresses. The orange line representing maximum temperature anywhere inside the cylinder at any given time takes a steep climb, momentarily reaching as high as 4200 K before plunging to less than 2400 K. However as is evident from the rising average temperature curve, the combustion isn't complete yet. This goes on to show that the max temperature exists at only a few locations inside the cylinder, which is not enough to influence the average temperature. However, pockets of high temperature

like these, are what responsible for production of NOx. Figure 19, shows the pressure plot. The pressure inside the cylinder is quite uniform, so just the average pressure is an accurate representation of development of pressure inside the cylinder.

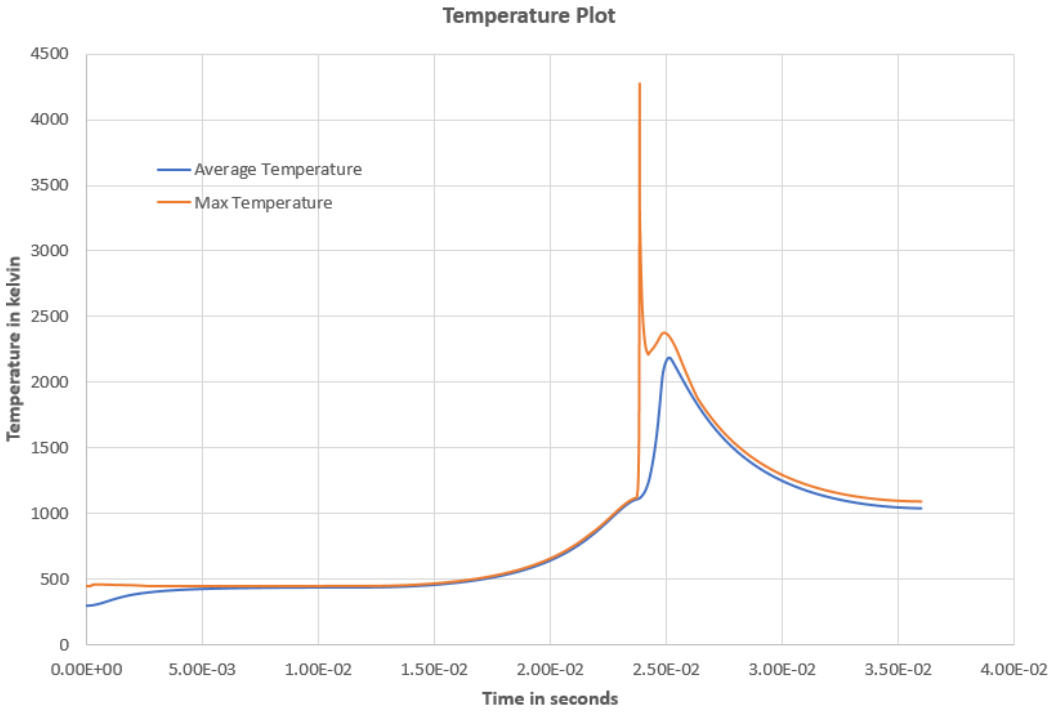

Fig. 18 Image shows Max and Average Temperature

HCCI is centered on an idea to increase efficiency and performance keeping emission production at low levels. Keeping that in mind we present the results in the Figure 20 for the formation of carbon mono-oxide (CO) and nitric oxide (NO). While production of CO is necessary for the combustion, NO is a byproduct of combustion under high temperature. Figure 20 is a time line of events occurring just after the onset of combustion. Below the 2.7e-2 seconds mark we see the temperature essentially remaining static with coincidental rise in concentration

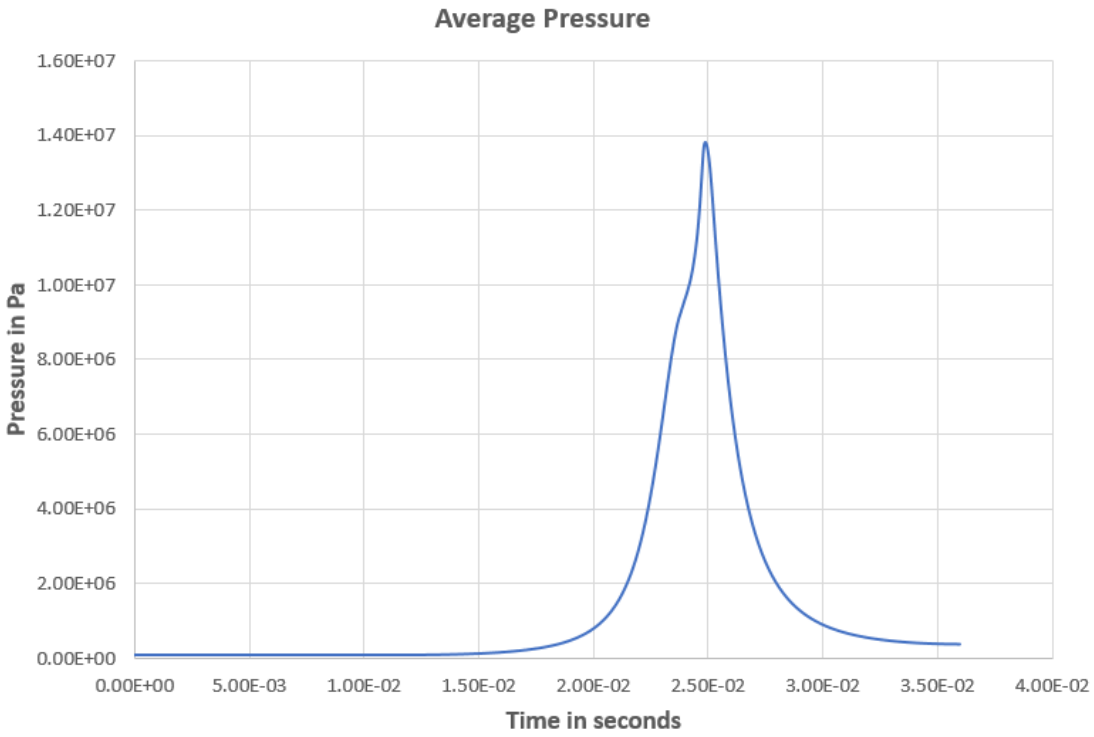

Fig. 19 Pressure plot

of CO; however, the concentration of NO remains low. After the 2.7e-2 seconds mark we observe a fall in temperature and an even sharper fall in concentration of CO. During this time however, we see rising level of NO concentration. After about 3.2e-2 seconds, the CO concentration is near zero and concentration of NO flattens out. The time between 2.7e-2 seconds and 3.2e-2 seconds is crucial because this is where all the emissions production takes place. In this phase of combustion, a higher temporal discretization is necessary to capture in greater detail the sequence of events.

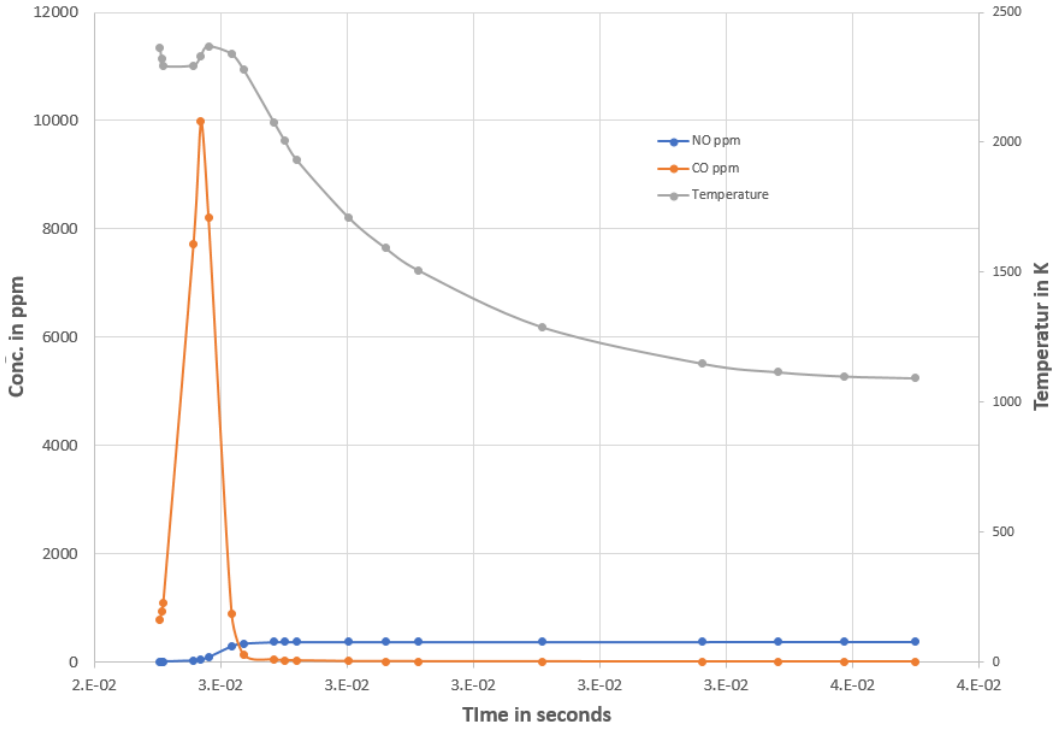

Fig. 20 Plot for production of CO and NO

4.3 Partially Completed 3D Result

Figure 21 shows the average heat transfer coefficient. The initial portion of the curve is negative as the temperature is inside the cylinder is lower than the wall the temperature; there is a negative heat flux in the cylinder. However, due to compression, when the temperature reaches above wall temperature, there is a net outflow of heat energy. Figure 22 shows the temperature plot. Note that the blue line is only given as a reference, it shows the ideal gas temperature at that time-step. However, the results from the CFD calculations are shown by the grey and red lines.

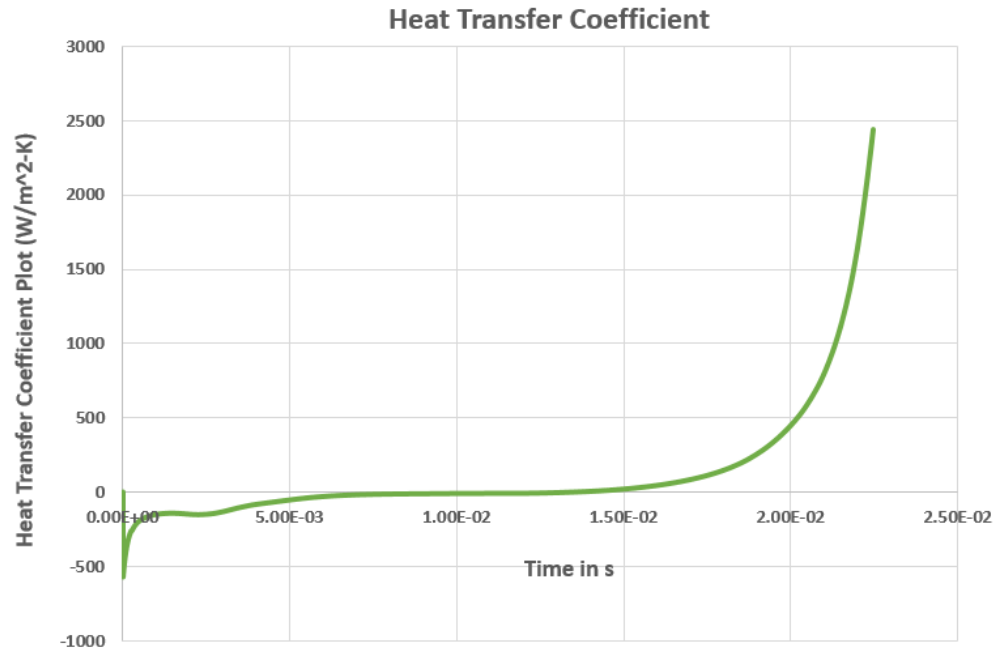

Fig. 21 Partially complete heat transfer plot

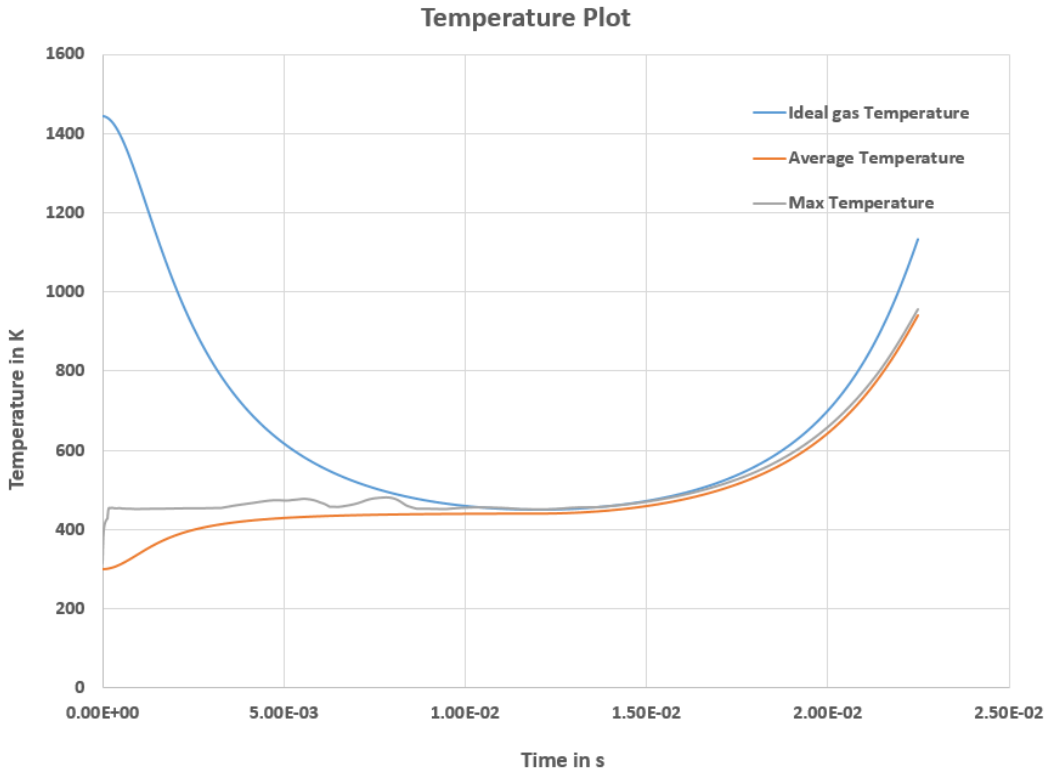

Fig. 22 Partially complete temperature plot

Chapter 5: CONCLUSION

5.1 Conclusion

In this work, a zero-dimensional along with a 2D axisymmetric model was developed to predict the temperature and formation of species due to compression ignition. The 0D model provides an inexpensive way to quickly realize effect of various parameters on combustion.

Simulink model simulates combustion using Wiebe function. Despite all its drawbacks, it has its usefulness once all the curve fit parameters have been determined with confidence. The chemical kinetics model on the other hand lets us make an educated guess as to the behavior of the HCCI engine. Following lists the conclusions derived from the model: -

- Fuel burn duration is extended at higher rpm.
- There is an optimum compression ratio at every rpm where compression ratio is at its highest.
- Unlike spark-ignition engines, higher compression ratio doesn't necessarily equate to higher work output.
- Slower burn corresponds to higher work output.

The CFD simulation gives us a more detailed view of the combustion. Estimation of concentration of oxides of nitrogen and carbon has been shown to form in detectable quantities. To achieve combustion, the intake temperature had to be increased to 450 K and the compression ratio to 18.4. So clearly, we see that this is quite a jump from the 300 K and 13 on the 0D model.

5.2 Future Work

In this study, the models have been developed with several assumptions to reduce the complexity. For instance, the 0D model uses a global one-step mechanism, which is not suitable for homogeneous reactor models. There is a delay in the start of ignition when the right conditions have been met; these models are not equipped to simulate that delay. Considering all these factors, the following list consolidates work that needs to be done to make the study more complete: -

- Use a multi-step reaction in the 0D model, which will better simulate the species formation.
- Work on HCCI is somewhat incomplete without studying the effects of EGR. EGR can be introduced in both the 0-D model and the CFD model.
- The CFD model doesn't consider surface chemistry. Since the cylinder surface is comparatively cool with respect to the interior, the products formed in this region are different from the ones within the cylinder. This surface chemistry gives rise to soot. Effect of cylinder walls can be introduced in the CFD model.
- This work focuses on lean mixtures; however, it is possible to use rich fuel mixtures. Introducing the water-gas equilibrium to 0-D model will help in simulating rich mixtures. There are complex chemistry models available for CFD, but complexity arises due to the need to calculate equilibrium between species at every time step.

References

Chang, J., Guralp, O., Filipi, Z., Assanis, D., Kuo, T.-W., Njt, P., & Rask, R. (2004). Transfer Correlation for the HCCI Engine Derived from Measurements of Instantaneous Surface Heat Flux. *Proceedings of the Society of Automotive Engineers*.

Christensen, M., Johansson, B., Amneus, P., & Mauss, F. (1998). Supercharged homogeneous charge compression ignition. *SAE Technical Paper 980787*.

Garcia, M., & Aguilar, F. (2009). A new heat release rate (HRR) law for homogeneous charge compression ignition (HCCI) combustion mode. *Applied Thermal Engineering*, 3654-3662.

Wang, Z., Shuai, S., Wang, J.-X., & Tian, G. (2006). A computational study of direct injection gasoline HCCI engine with secondary injection. *Fuel, 85*(12-13), 1831-1841.

Woschi, G. (1967). A universally applicable equation for the Instantaneous Heat Transfer Coefficient in the Internal Combustion Engine. *Proceedings of the Society of Automotive Engineers*, 3065-3083.

Yeliana, Y., Cooney, C., Worm, J., Michalek, D. J., & Naber, D. J. (2006). Estimation of double-Wiebe function parameters using least square method for burn durations or ethanol-gasoline blends in spark ignition engines over variable compression and EGR levels. *Applied Thermal Engineering*, 2213-2220.

Zhang, Z. Y., Kung, E. H., & Haworth, D. C. (2005). A PDF method for multidimensional modeling of HCCI engine combustion: effects of turbulence/chemistry interactions on ignition timing and emissions. *Proceedings of the Combustion Institute*, 2763-2771.